Optics Letters

Wavelength division multiplexed light source monolithically integrated on a silicon photonics platform

Purnawirman,[1] Nanxi Li,[1,2,*] E. Salih Magden,[1] Gurpreet Singh,[1] Michele Moresco,[1] Thomas N. Adam,[3] Gerard Leake,[3] Douglas Coolbaugh,[3] Jonathan D. B. Bradley,[1,4] and Michael R. Watts[1]

[1]Photonic Microsystems Group, Research Laboratory of Electronics, Massachusetts Institute of Technology, 77 Massachusetts Avenue, Cambridge, Massachusetts 02139, USA
[2]John A. Paulson School of Engineering and Applied Sciences, Harvard University, 29 Oxford Street, Cambridge, Massachusetts 02138, USA
[3]College of Nanoscale Science and Engineering, University at Albany, State University of New York, 257 Fuller Road, Albany, New York 12203, USA
[4]Currently at Department of Engineering Physics, McMaster University, 1280 Main Street West, Hamilton, Ontario L8S 4L7, Canada
*Corresponding author: nanxili@mit.edu

Received 23 February 2017; accepted 31 March 2017; posted 7 April 2017 (Doc. ID 287189); published 25 April 2017

We demonstrate monolithic integration of a wavelength division multiplexed light source for silicon photonics by a cascade of erbium-doped aluminum oxide (Al_2O_3:Er^{3+}) distributed feedback (DFB) lasers. Four DFB lasers with uniformly spaced emission wavelengths are cascaded in a series to simultaneously operate with no additional tuning required. A total output power of −10.9 dBm is obtained from the four DFBs with an average side mode suppression ratio of 38.1 ± 2.5 dB. We characterize the temperature-dependent wavelength shift of the cascaded DFBs and observe a uniform $d\lambda/dT$ of 0.02 nm/°C across all four lasers.

OCIS codes: (130.0130) Integrated optics; (130.3120) Integrated optics devices; (140.3460) Lasers.

https://doi.org/10.1364/OL.42.001772

A wavelength division multiplexed (WDM) light source is a key component in silicon photonics technology for application in optical communications [1–3]. It generally consists of several uniformly spaced optical wavelengths that can be used to encode multiple communication channels in a common output. Several research groups have demonstrated integrated WDM light sources of up to 16 channels by bonding of III-V gain material onto the silicon chip [4–8]. However, these hybrid devices often require careful temperature control and complex fabrication steps with yield challenges. Alternatively, rare-earth-doped glass lasers on silicon, such as erbium-doped aluminum oxide (Al_2O_3:Er^{3+}) or thulium-doped aluminum oxide (Al_2O_3:Tm^{3+}) lasers, have been shown to achieve high power, low noise, good thermal stability, and low lasing threshold [9–13]. Monolithic integration of Al_2O_3:Er^{3+} lasers has been demonstrated in a CMOS-compatible process with only a single backend Al_2O_3:Er^{3+} deposition step [14–16]. The wide gain bandwidth of the erbium enables the laser wavelength tunability and design flexibility [17–22]. By combining several lasers with varying grating periods, a multi-wavelength light source can be obtained with custom longitudinal mode spacing.

In this Letter, we demonstrate a monolithic WDM source by cascading four Al_2O_3:Er^{3+} distributed (DFB) lasers. We achieve simultaneous operation of four DFBs at a total power of −10.9 dBm and an average side mode suppression ratio (SMSR) of 38.1 ± 2.5 dB in each DFB. The measured temperature-dependent wavelength shift is uniform across all four lasers with $d\lambda/dT = 0.02$ nm/°C.

The design of the cascaded DFB structure is shown in Fig. 1. Four DFB lasers are cascaded in a series with the length of each laser $L_{DFB} = 5.5$ mm, the distance between each laser $L_{spacing} = 0.1$ mm, and the first grating period $\Lambda_1 = 490$ nm with 2 nm subsequent increment ($\Lambda_2 = 492$ nm, $\Lambda_3 = 494$ nm, and $\Lambda_4 = 496$ nm). Each DFB laser has a quarter phase shift located at the center, thus emitting symmetric outputs on both sides. The right output from DFB_1 propagates to the next laser DFB_2, and so on to the right end of the structure. The combined output is then a WDM of four uniformly spaced wavelengths. In order to design an asymmetric output that emits on only one end of the device, the phase shift can be placed to be slightly off-center in the cavity. With small reabsorption loss (0.5 dB/cm at 1563 nm [23]) and good thermal stability of the Al_2O_3:Er^{3+} laser, the lasers can be placed closely with negligible crosstalk.

In order to allow integration into a more general silicon photonics wafer-scale process where thicker, higher-confinement silicon nitride (SiN_x) structures might be preferred [24], we extend our erbium laser design [10] to work for a thicker SiN_x by using a multi-segmented waveguide structure [25,26]. To form a compact CMOS-compatible cascaded DFB structure, we optimized the multi-segmented waveguide design for short lasers. Figure 2 shows the laser waveguide

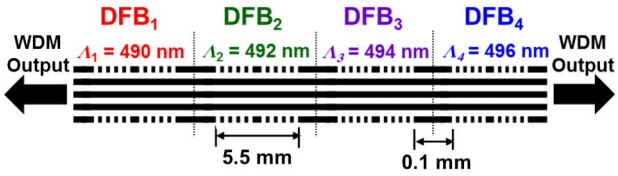

Fig. 1. Design of a WDM light source by cascaded DFBs. Four $Al_2O_3:Er^{3+}$ DFB lasers at a uniformly spaced grating period are cascaded in a series to generate a multi-wavelengths laser output.

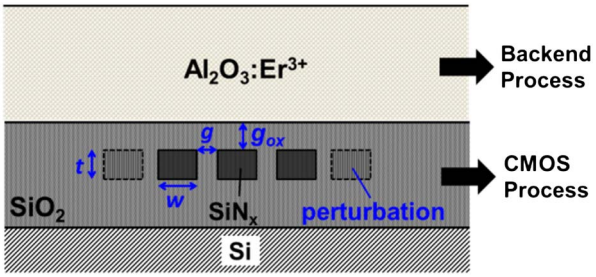

Fig. 2. CMOS-compatible multi-segmented waveguide design of $Al_2O_3:Er^{3+}$ DFB lasers. The structure consists of five SiN_x segments used for a thicker SiN_x design, with the grating constructed by periodic perturbation of the outer segments.

which consists of nitride (SiN_x) segments with the grating perturbation formed by periodic etching of the first and last segments. The SiN_x segments have dimensions of thickness $t = 200$ nm, width $w = 450$ nm, and gap $g = 400$ nm. A silicon dioxide (SiO_2) gap $g_{ox} = 200$ nm is then added on top of the SiN_x structure. All fabrication steps until SiO_2 cladding are completed in a 300 mm line CMOS foundry, as reported earlier [10], only with a difference in layer thickness. Lastly, the $Al_2O_3:Er^{3+}$ gain medium of thickness $t_{AlO} = 1100$ nm is deposited by a reactive co-sputtering process [23,27] as the final backend step. The Er^{3+} ion concentration is $N_{Er} = 1.0 \times 10^{20}$ cm^{-3}, and the background loss is measured to be <0.1 dB/cm, using the prism coupling method.

The multi-segmented waveguide is designed to have a single transverse-electric mode at the pump (980 nm) and laser (1550 nm) wavelengths. The design also allows for efficient optical pumping of the $Al_2O_3:Er^{3+}$ lasers with high mode confinement and good intensity overlap of the pump and laser mode. The confinement factor of the pump and laser in the gain layer is calculated using a finite difference mode solver to be 89% and 90%, respectively, with an intensity overlap >95%, as shown in Fig. 3.

We measure the transmission response of the cascaded DFB structure by using a tunable laser, as shown in Fig. 4. Sharp resonances are located at the center of each DFB response at wavelengths $\lambda_1 = 1563.56$ nm, $\lambda_2 = 1569.84$ nm, $\lambda_3 = 1575.90$ nm, and $\lambda_4 = 1581.76$ nm. The sharp peaks have a lower transmission amplitude (10–15 dB) in the passive measurement of $Al_2O_3:Er^{3+}$, mainly due to the absorption of an unpumped active ion. The wavelength spacings between adjacent DFBs are slightly nonuniform ($\Delta\lambda_{adjacent} = 6.28$, 6.06, and 5.86 nm). We believe that this can be explained by the

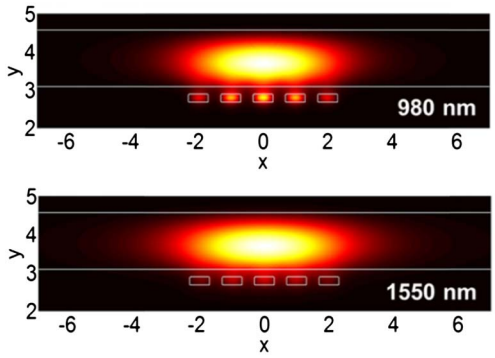

Fig. 3. Mode solver calculation of the intensity distribution for the pump (980 nm) and laser (1550 nm) wavelengths in the multi-segmented waveguide design.

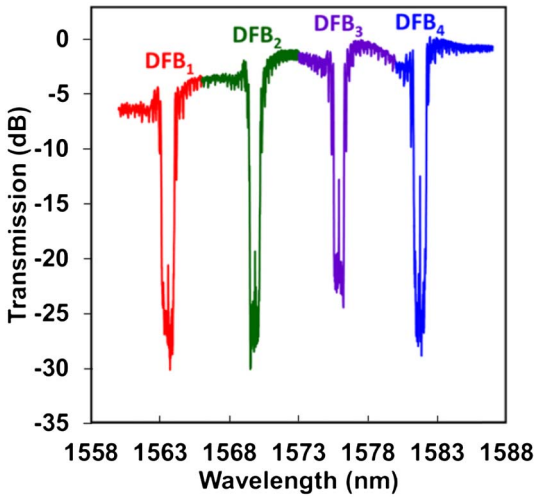

Fig. 4. Transmission measurement of a cascaded DFB structure. The sharp peaks have a lower transmission amplitude (10–15 dB) in the passive measurement of $Al_2O_3:Er^{3+}$, mainly due to the absorption of an unpumped active ion.

thickness nonuniformity of the $Al_2O_3:Er^{3+}$ film deposition. In a standard sputtering system, the target is mounted on a rotating platform with a radially varying thickness profile from the center. Thus, a conventional straight DFB structure would experience thickness nonuniformity along the cavity. We present a more detailed explanation and a possible solution in a follow-up work [28].

Laser measurements were carried out by pumping the cascaded DFB structure from both sides with two fiber pigtailed laser diodes centered at 978 (left side) and 976 nm (right side). Accounting for fiber chip coupling losses, the maximum on-chip pump powers of the 978 and 976 nm diodes are estimated to be 120 mW (left pump) and 70 mW (right pump), respectively. The output is monitored using two optical spectrum analyzers (OSAs) on both sides. We obtain laser wavelengths centered at 1563.92, 1570.20, 1576.28, and 1582.16 nm, slightly higher than the passive transmission measurement due to local heating by pump absorption. The peak output powers obtained in the left (and right) OSA for the four

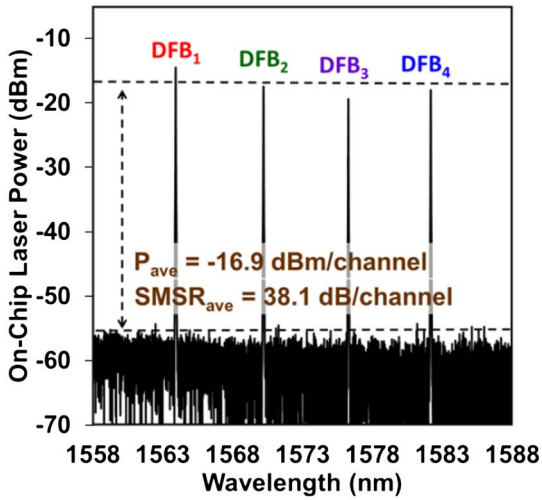

Fig. 5. Total emission spectrum of the cascaded DFB WDM source at a maximum pump power.

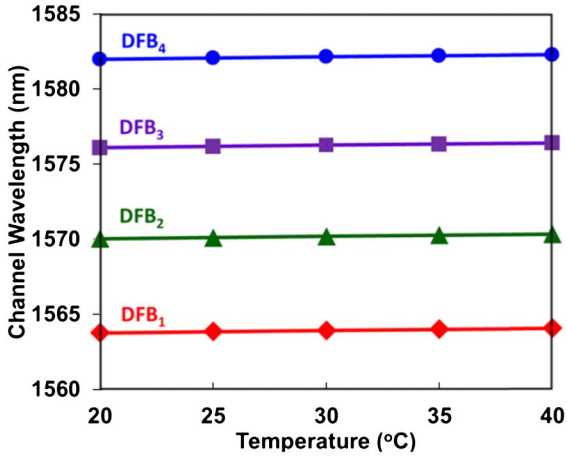

Fig. 7. Temperature-dependent wavelength shift of lasers in a cascaded DFB structure shows gradual changes in 20°C–40°C (0.02 nm/°C) and uniformity across all channels.

DFBs are as follows: −17.7 (−17.4 dBm), −20.4 (−20.2 dBm), −22.1 (−22.6 dBm), and −19.1 dBm (−24.0 dBm). The measured power from the left and right OSA generally show similar output levels, except for DFB_4, which might be caused by a fabrication defect. We plot the total emission spectrum of the cascaded DFBs by adding the spectrum obtained from both left and right OSAs in Fig. 5. The total peak power obtained for different wavelengths are −14.5, −17.5, −19.4, and −18.0 dBm. This corresponds to a total cascaded DFB output power of −10.9 dBm from all four DFBs, an average of −16.9 dBm per DFB. By assuming the noise floor at −55.0 dBm, as shown in the figure, we obtain an average of 38.1 ± 2.5 dB SMSR per DFB which, to the best of our knowledge, is one of the best signal-to-noise performances of an on-chip WDM light source ever reported [6].

We perform a temperature dependence test of the cascaded DFBs by placing the chip on a thermoelectric cooler (TEC). The TEC temperature can be adjusted from 20°C to 40°C by varying the current level. Figure 6 shows the spectrum of

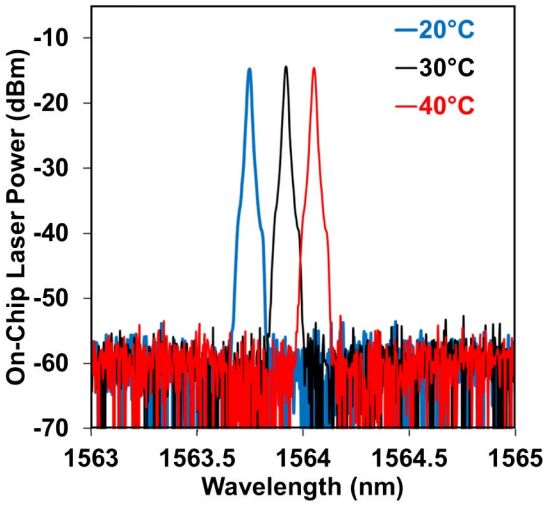

Fig. 6. OSA spectra of DFB_1 laser at varying temperatures, from 20°C to 40°C, showing $d\lambda/dT$ of 0.02 nm/°C.

DFB_1 at temperatures of 20°C, 30°C, and 40°C. No significant change of the output power is observed at varying temperatures, demonstrating thermal stability of the Al_2O_3:Er^{3+} lasers. Figure 7 shows the wavelengths of all four DFBs at varying temperatures with a uniform temperature-dependent shift of $d\lambda/dT = 0.02$ nm/°C across all four lasers. This is less than half, compared with the thermal wavelength shift of the hybrid lasers for WDM [5,6,29,30].

Improved performance of the cascaded DFB laser WDM light source can be achieved in the following ways. The maximal output of each DFB laser can be optimized by varying the grating strength κ and cavity length L_{DFB}, as shown in [15]. The pump laser can be recirculated by using a selective reflector to obtain a more flattened spatial pump profile. In addition, by taking into account the doping concentration, reabsorption loss, and total available pump power, the combined WDM output can be carefully designed to have better power uniformity. Lastly, to scale the cascaded DFB to include more DFB lasers, several structures can be combined in parallel, or the structure can be folded around the chip to increase the total available length. (Here the design was constrained by the chip length of 2.5 cm.)

In summary, we have demonstrated CMOS-compatible monolithic integration of a WDM light source in a silicon photonics platform by a cascade of Al_2O_3:Er^{3+} DFB lasers. Simultaneous operation of four DFB lasers has been achieved with a total power of −10.9 dBm, corresponding to an average power of −16.9 dBm and a 38.1 ± 2.5 dB SMSR for each DFB laser. The output shows good thermal stability with varying chip temperatures (20°C–40°C), with a uniform temperature-dependent wavelength shift of $d\lambda/dT = 0.02$ nm/°C across all four DFBs. We propose that such Al_2O_3:Er^{3+} lasers are an alternative approach to low noise and thermally stable WDM light sources for optical communications.

Funding. Defense Advanced Research Projects Agency (DARPA) (HR0011-12-2-0007).

Acknowledgment. The authors would like to acknowledge Dr. Joshua Conway for the helpful discussions.

N. Li is sponsored by National Science Scholarship (NSS) from the Agency of Science, Technology and Research (A*STAR), Singapore.

REFERENCES

1. M. J. R. Heck, J. F. Bauters, M. L. Davenport, J. K. Doylend, S. Jain, G. Kurczveil, S. Srinivasan, Y. B. Tang, and J. E. Bowers, IEEE J. Sel. Top. Quantum Electron. **19**, 6100117 (2013).
2. L. Stampoulidis, K. Vyrsokinos, K. Voigt, L. Zimmermann, F. Gomez-Agis, H. J. S. Dorren, Z. Sheng, D. Van Thourhout, L. Moerl, J. Kreissl, B. Sedighi, J. C. Scheytt, A. Pagano, and E. Riccardi, IEEE J. Sel. Top. Quantum Electron. **16**, 1422 (2010).
3. M. J. R. Heck, H. W. Chen, A. W. Fang, B. R. Koch, D. Liang, H. Park, M. N. Sysak, and J. E. Bowers, IEEE J. Sel. Top. Quantum Electron. **17**, 333 (2011).
4. A. Alduino, L. Liao, R. Jones, M. Morse, B. Kim, W.-Z. Lo, J. Basak, B. Koch, H.-F. Liu, H. Rong, M. Sysak, C. Krause, R. Saba, D. Lazar, L. Horwitz, R. Bar, S. Litski, A. Liu, K. Sullivan, O. Dosunmu, N. Na, T. Yin, F. Haubensack, I.-W. Hsieh, J. Heck, R. Beatty, H. Park, J. Bovington, S. Lee, H. Nguyen, H. Au, K. Nguyen, P. Merani, M. Hakami, and M. Paniccia, *Integrated Photonics Research, Silicon and Nanophotonics (IPRSN)* (2010).
5. S. S. Sui, M. Y. Tang, Y. D. Yang, J. L. Xiao, Y. Du, and Y. Z. Huang, IEEE J. Quantum Electron. **51**, 1 (2015).
6. S. Tanaka, S. H. Jeong, S. Sekiguchi, T. Akiyama, T. Kurahashi, Y. Tanaka, and K. Morito, in *Optical Fiber Communication Conference and Exposition and the National Fiber Optic Engineers Conference* (IEEE, 2013).
7. L. Tao, L. Yuan, Y. Li, H. Yu, B. Wang, Q. Kan, W. Chen, J. Pan, G. Ran, and W. Wang, Opt. Express **22**, 5448 (2014).
8. G. Kurczveil, M. J. R. Heck, J. D. Peters, J. M. Garcia, D. Spencer, and J. E. Bowers, IEEE J. Sel. Top. Quantum Electron. **17**, 1521 (2011).
9. N. Li, Purnawirman, Z. Su, E. Salih Magden, P. T. Callahan, K. Shtyrkova, M. Xin, A. Ruocco, C. Baiocco, E. P. Ippen, F. X. Kärtner, J. D. B. Bradley, D. Vermeulen, and M. R. Watts , Opt. Lett. **42**, 1181 (2017).
10. E. S. Hosseini, Purnawirman, J. D. B. Bradley, J. Sun, G. Leake, T. N. Adam, D. D. Coolbaugh, and M. R. Watts, Opt. Lett. **39**, 3106 (2014).
11. E. H. Bernhardi, H. van Wolferen, L. Agazzi, M. R. H. Khan, C. G. H. Roeloffzen, K. Worhoff, M. Pollnau, and R. M. de Ridder, Opt. Lett. **35**, 2394 (2010).
12. M. Belt and D. J. Blumenthal, in *Optical Fiber Communications Conference and Exhibition* (2015), pp. 1–3.
13. Z. Su, N. Li, E. Salih Magden, M. Byrd, Purnawirman, T. N. Adam, G. Leake, D. Coolbaugh, J. D. B. Bradley, and M. R. Watts, Opt. Lett. **41**, 5708 (2016).
14. G. Singh, Purnawirman, J. D. B. Bradley, N. Li, E. S. Magden, M. Moresco, T. N. Adam, G. Leake, D. Coolbaugh, and M. R. Watts, Opt. Lett. **41**, 1189 (2016).
15. M. Belt and D. J. Blumenthal, Opt. Express **22**, 10655 (2014).
16. E. S. Magden, Purnawirman, N. Li, G. Singh, J. D. B. Bradley, G. S. Petrich, G. Leake, D. D. Coolbaugh, M. R. Watts, and L. A. Kolodziejski, "Fully CMOS-compatible integrated distributed feedback laser with 250°C fabricated Al_2O_3:Er^{3+} gain medium," in *Conference on Lasers and Electro-Optics (CLEO)*, San Jose, California, Optical Society of America, 2016, paper SM1G.2.
17. Y. Liu, K. Wu, N. Li, L. Lan, S. Yoo, X. Wu, P. P. Shum, S. Zeng, and X. Tan, J. Opt. Soc. Korea **17**, 357 (2013).
18. N. J. C. Libatique, L. Wang, and R. K. Jain, Opt. Express **10**, 1503 (2002).
19. N. Li, E. Timurdogan, C. V. Poulton, M. Byrd, E. S. Magden, Z. Su, Purnawirman, G. Leake, D. D. Coolbaugh, D. Vermeulen, and M. R. Watts, Opt. Express **24**, 22741 (2016).
20. Y. W. Song, S. A. Havstad, D. Starodubov, Y. Xie, A. E. Willner, and J. Feinberg, IEEE Photon. Technol. Lett. **13**, 1167 (2001).
21. J. H. Wong, H. Q. Lam, S. Aditya, J. Zhou, N. Li, J. Xue, P. H. Lim, K. E. K. Lee, K. Wu, and P. P. Shum, J. Lightwave Technol. **30**, 3164 (2012).
22. F. Xiao, K. Alameh, and T. Lee, Opt. Express **17**, 18676 (2009).
23. K. Worhoff, J. D. B. Bradley, F. Ay, D. Geskus, T. P. Blauwendraat, and M. Pollnau, IEEE J. Quantum Electron. **45**, 454 (2009).
24. A. Gondarenko, J. S. Levy, and M. Lipson, Opt. Express **17**, 11366 (2009).
25. Purnawirman, E. S. Hosseini, J. Sun, T. N. Adam, G. Leake, D. D. Coolbaugh, M. R. Watts, and A. Baldycheva, in *Optical Fiber Communication Conference*, San Francisco, California, 2014, paper W4E.5.
26. C. M. Sorace-Agaskar, P. T. Callahan, K. Shtyrkova, A. Baldycheva, M. Moresco, J. Bradley, M. Y. Peng, N. Li, E. S. Magden, P. Purnawirman, M. Y. Sander, G. Leake, D. Coolbaugh, M. R. Watts, and F. Kartner, "Integrated mode-locked lasers in a CMOS-compatible silicon photonic platform," in *Conference on Lasers and Electro-Optics (CLEO)*, San Jose, California, Optical Society of America, 2015, paper SM2I.5.
27. J. D. Bradley, Z. Su, E. S. Magden, N. Li, M. Byrd, Purnawirman, T. N. Adam, G. Leake, D. Coolbaugh, and M. R. Watts, Proc. SPIE **9744**, 97440U (2016).
28. Purnawirman, "Integrated erbium lasers in silicon photonics," Ph.D. dissertation (Massachusetts Institute of Technology, 2017).
29. S. Tanaka, S.-H. Jeong, S. Sekiguchi, T. Kurahashi, Y. Tanaka, and K. Morito, Opt. Express **20**, 28057 (2012).
30. J. Seok-Hwan, T. Shinsuke, S. Shigeaki, K. Teruo, H. Nobuaki, A. Suguru, U. Tatsuya, Y. Tsuyoshi, A. Tomoyuki, T. Yu, and M. Ken, Jpn. J. Appl. Phys. **51**, 082101 (2012).